Published online 29 April 2016

Nucleic Acids Research, 2016, Vol. 44, No. 15 ***7219–7227***
doi: 10.1093/nar/gkw352

DNA compaction by the bacteriophage protein Cox studied on the single DNA molecule level using nanofluidic channels

Karolin Frykholm[1], Ronnie Per-Arne Berntsson[2], Magnus Claesson[2], Laura de Battice[3], Richard Odegrip[4], Pål Stenmark[2,*] and Fredrik Westerlund[1,*]

[1]Department of Biology and Biological Engineering, Chalmers University of Technology, SE-41296 Gothenburg, Sweden, [2]Department of Biochemistry and Biophysics, Arrhenius Laboratories for Natural Sciences, Stockholm University, SE-10691 Stockholm, Sweden, [3]Department of Chemistry and Chemical Engineering, Chalmers University of Technology, SE-41296 Gothenburg, Sweden and [4]Department of Molecular Biosciences, The Wenner-Gren Institute, Arrhenius Laboratories for Natural Sciences, Stockholm University, SE-10691 Stockholm, Sweden

Received October 08, 2015; Revised March 17, 2016; Accepted March 30, 2016

ABSTRACT

The Cox protein from bacteriophage P2 forms oligomeric filaments and it has been proposed that DNA can be wound up around these filaments, similar to how histones condense DNA. We here use fluorescence microscopy to study single DNA–Cox complexes in nanofluidic channels and compare how the Cox homologs from phages P2 and WΦ affect DNA. By measuring the extension of nanoconfined DNA in absence and presence of Cox we show that the protein compacts DNA and that the binding is highly cooperative, in agreement with the model of a Cox filament around which DNA is wrapped. Furthermore, comparing microscopy images for the wild-type P2 Cox protein and two mutants allows us to discriminate between compaction due to filament formation and compaction by monomeric Cox. P2 and WΦ Cox have similar effects on the physical properties of DNA and the subtle, but significant, differences in DNA binding are due to differences in binding affinity rather than binding mode. The presented work highlights the use of single DNA molecule studies to confirm structural predictions from X-ray crystallography. It also shows how a small protein by oligomerization can have great impact on the organization of DNA and thereby fulfill multiple regulatory functions.

INTRODUCTION

P2-like phages are temperate phages that infect *Escherichia coli* and bacteriophage P2 is seen as the prototype of the P2-like family of phages found in γ-proteobacteria (1). A phage closely related to P2, namely WΦ, has been isolated from *E. coli* W, where it restricts the growth of phage λ. Basically all P2-like phages have a similar organization of the transcriptional switch, containing the Pe and Pc promotors, located face-to-face, and the immunity repressor C and the lytic repressor Cox, which recognize different operators (2,3).

The small, 91 residues long, Cox protein of phage P2 is multi-functional; (i) it plays a role in the excision of the P2 prophage (4), (ii) it transcriptionally represses the P2 Pc promotor (5) and (iii) it transcriptionally activates the satellite phage P4 P_{LL} promotor (6). Phage P4 depends on P2 for lytic growth. Cox from WΦ (90 aa), on the other hand, has been shown to repress the WΦ Pc promotor and to promote excision *in vitro* (7), but does not activate the P4 satellite phage (8).

P2 Cox binds, in a cooperative manner, to so called cox-boxes on the DNA, which has a sequence of TTAAA(G/C)NC(A/C) (7). These cox-boxes are directional, and basically provide a footprint to where, and in which direction, P2 Cox should bind to the DNA. At higher protein concentrations, P2 Cox also binds to non-specific nucleotide sequences, likely also here in a cooperative manner (9). WΦ Cox does not bind to those cox-boxes, but instead recognizes a direct repeat of 12 nucleotides that is found in the WΦ Pe-Pc region (7). We recently determined the structure of P2 Cox (10), which showed that it oligomerizes in a helical fashion, forming a left-handed filament with a diameter of ∼65Å and a rise

*To whom correspondence should be addressed. Tel: +46 31 772 3049; Fax: +46 31 772 3858; Email: fredrik.westerlund@chalmers.se
Correspondence may also be addressed to Pål Stenmark. Tel: +46 8 163729; Fax: +46 8 153679; Email: stenmark@dbb.su.se
Present address: Ronnie Per-Arne Berntsson, Department of Medical Biochemistry and Biophysics, Umeå University, SE-90187 Umeå, Sweden.

of ∼34Å, with its DNA binding helix and wing pointing outward (Figure 1). This indicates a possibility for the Cox oligomer to bind DNA in a way highly similar to how histone particles wind up DNA around themselves in nucleosomes. From previous work it was clear that both P2 Cox and WΦ Cox strongly bend DNA upon binding and that they protect large stretches of DNA from DNAse I cleavage (4,5,7). Based on the structure, together with previous biochemical and genetical work, we postulated that P2 Cox achieves its different functions by wrapping the DNA around its own oligomer in a helical fashion (Figure 1) (10). By doing this it would either expose stretches of DNA, as in the case of the activation of P4, or protect stretches of DNA, as in the case of repression of the P2 Pc promotor and, as proposed, for excision of P2.

Less is known about the function of WΦ Cox. However, the sequence identity and similarity to P2 Cox are 37% and 58%, respectively. Secondary structure predictions show that WΦ Cox has the same secondary structure organization as P2 Cox. From sequence alignment it is also clear that WΦ Cox has the same C-terminal organization as P2 Cox, indicating that WΦ Cox oligomerizes in a similar fashion as P2 Cox. Furthermore, it has been suggested that at increased WΦ Cox concentrations, it binds cooperatively also to non-specific nucleotide sequences, which might indicate the formation of a filament (7). Based on this it is therefore likely that the function and DNA binding of WΦ Cox is similar to that of P2 Cox.

Nanofluidic channels have emerged as a useful complement to existing techniques for investigating single DNA molecules (11,12). Applications include, among others, fundamental studies of the polymer physics of confined DNA (13) and optical DNA mapping (14,15). DNA–protein interactions have been less explored, but significant progress has been made during the last 5 years. An important breakthrough for such studies was the demonstration of lipid bilayers as being perfectly suited for passivating the channel walls to avoid non-specific interactions (16). This has led to several studies in recent years investigating how proteins affect the physical properties of DNA (17–20). Examples include studies of the persistence length of stiff RecA filaments (20) and of the mechanism by which Hfq compacts DNA (18).

Our structural model of P2 Cox implies that a DNA-Cox filament would be significantly less extended than the corresponding naked DNA. To test this hypothesis, we in this study stretch DNA–Cox complexes in nanofluidic channels. We demonstrate that Cox indeed compacts DNA and that the binding is highly cooperative. This agrees well with the fact that Cox forms filaments around which DNA can wrap itself. We compare how the two homologs, P2 Cox and WΦ Cox, affect DNA, and find that they both have a similar effect on the DNA extension, suggesting similar binding modes. However, WΦ Cox has a slightly higher binding affinity to DNA, as judged by a more efficient compaction of DNA, indicating subtle differences in DNA binding between the two proteins. Using two P2 Cox mutants we also demonstrate that we can discriminate between compaction due to filament formation and compaction by monomeric Cox; both are present for the wild-type protein. The physical properties of the DNA are not affected at low amounts of protein bound but the DNA–protein complex becomes stiff at higher protein loads, as the Cox filament presumably grows to accommodate the whole DNA molecule.

MATERIALS AND METHODS

Protein expression and purification

WΦ Cox was expressed in *E. coli* BL21(DE3) pLysS (21) containing plasmid pEE901 (8). The bacteria were grown in LB medium in an LEX bubbling system (SGC) at 37°C until OD600 0.6 when isopropyl-β-D-thiogalactopyranoside (IPTG) was added to a final concentration of 0.5 mM. The culture was allowed to grow overnight at 22°C until harvested by centrifugation. The pellet was resuspended in 0.3 M potassium phosphate buffer, pH 7.5, 3 mM EDTA, 0.5 M KCl, 0.1% Triton at 6 ml per gram of cells and freeze thawed twice to allow leakage of lysozyme and partial lysis. To complete lysis, resuspended cells were sonicated on ice in four 30-s bursts at 12–14 μm with an MSE Soniprep 150. The extract was clarified by centrifugation in a Sorvall RC5C at 23 000 × *g* for 1 h at 4°C and ammonium sulfate was added to 35% saturation to the supernatant. After being gently stirred at 4°C for 1 h, the mixture was centrifuged at 17 000 × *g* for 30 min, and the pellet was subsequently resuspended in 10 mM potassium phosphate buffer, pH 7.5, 3 mM EDTA, 150 mM KCl followed by filtration through 0.45 μm and 0.22 μm filters. The extract was loaded on a HiTrap 5 ml Heparin column (GE Healthcare) and eluted with a gradient of 10 mM potassium phosphate buffer, pH 7.5, 3 mM EDTA, 1 M KCl over ten column volumes. The WΦ Cox-containing fractions were analyzed by 20% homogenous SDS-PAGE gels using the PhastSystem (GE Healthcare) and concentrated to 890 μM using Vivaspin Centrifugal Concentrator (Vivaproducts), flash frozen in liquid nitrogen and stored at −80°C.

P2 Cox was expressed and purified as previously described (10). Briefly, the procedure was the same as for WΦ Cox, but with an added final purification step using size-exclusion chromatography. The protein (in 20 mM Tris-HCl pH 7.5, 150 mM NaCl, 15% isopropanol and 0.5 mM TCEP) was concentrated to 90 μM, flash-frozen in liquid nitrogen and stored at −80°C.

The pEE720 derivatives, described in (10) , encoding the sequences of the P2 Cox mutants R29A and Y70stop were transformed into E. coli(DE3) Rosetta, pLysS. The bacteria were grown in TB media in a LEX bubbling system (SGC) at 37°C until OD600 2.2 when IPTG was added to a final concentration of 0.5 mM. The respective cultures were incubated for an additional 16 h at 20°C prior to harvesting by centrifugation. The resulting pellets were resuspended in lysis buffer (0.1 M potassium phosphate, pH 7.5, 0.5 M KCl, 0.1 % (v/v) Triton-X100, supplemented with complete protease inhibitors (Roche), DNAseI (Applichem) and lysozyme (Applichem)) and incubated at room temperature for 30 min. The by centrifugation (125,000 × g, 4°C, 40 min) clarified lysates were filtered through 0.45 and 0.22 μm filters. Saturated ammonium sulphate solution was slowly added to the respective filtrates to final concentrations of 25 and 30% (v/v) for R29A and Y70stop respectively, and incubated for 30 min at 4°C. The precipitated material was fractionated by centrifugation (125,000 × g,

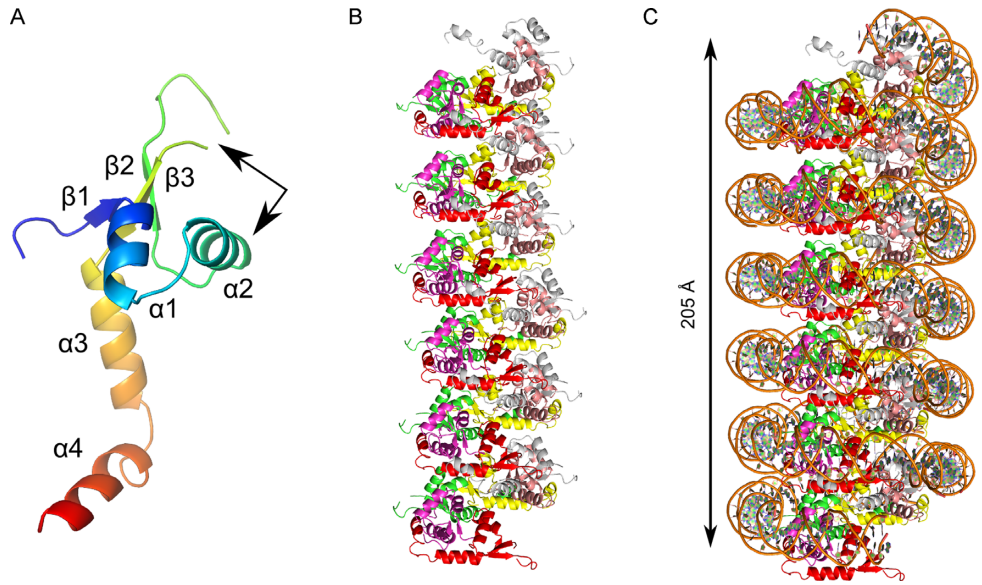

Figure 1. Structural model of P2 Cox binding to DNA. (**A**) Cartoon representation of P2 Cox, colored blue to red from the N- to the C-terminal. The DNA-binding helix and wing are marked with arrows and the secondary structure elements are indicated. (**B**) A view of how 36 P2 Cox monomers form a filament of 6 turns. (**C**) The same 6 turn filament of P2 Cox as in (B), but here in a model of how it wraps DNA around itself. The distance between two P2 Cox proteins 6 turns apart is ∼205 Å, thus ∼34 Å per turn.

4°C, 30 min) and the respective mutants were retrieved in the pellets and resuspended in 10 mM potassium phosphate buffer, pH 7.5, 0.1 M KCl, 15 % (v/v) isopropanol, prior to heparin column purification (HiPrep Heparin FF 16/60, GE healthcare) where the respective mutants were collected from the flow through. The Y70stop mutant was further purified by anion exchange (HiTrap Q FF, GE Healthcare) in 20 mM Tris pH 7.5, 0.1 M NaCl, 15 % (v/v) isopropanol, with the mutant recovered from the flow through. For both mutants the final purification step was size-exclusion chromatography (s200, 16/60, GE Healthcare, in 20 mM Tris pH 7.5, 0.15 M NaCl, 15 % (v/v) isopropanol, 0.5 mM TCEP)). The fractions containing the respective purified mutants Y29A and Y70stop were individually pooled and concentrated (VivaSpin, 10 kDa MWCO, 20°C, GE Healthcare) to 90 and 36.5 μM, prior to flash freezing in liquid nitrogen.

Nanofluidics

The single DNA molecule experiments were performed in funnel-shaped nanochannels with a width ranging from 100 to 800 nm and a depth of 140 nm. The devices were fabricated using advanced nanofabrication as described elsewhere (12) and consist of a pair of microchannels, spanned by funnel-shaped nanochannels (Figure 2A). The sample is introduced into the channel system via one of the four reservoirs that are connected to the microchannels and moved inside the channels by flow induced by applying pressure on the reservoir inlets of the microchannels. The funnel set-up allows for studies of the same molecule at different positions, with varying channel widths, along the nanofunnel (22).

To avoid non-specific binding of protein to the negatively charged channels walls, the channels were prior to sample introduction coated with a lipid bilayer comprising 99% 1-palmitoyl-2-oleoyl-sn-glycero-3-phosphocholine (POPC, Avanti) and 1% lissamine rhodamine B 1,2-dihexadecanoyl-sn-glycero-3-phosphoethanolamine, triethylammonium salt, (rhodamine-DHPE, Invitrogen). The coating procedure is described in detail in (16).

DNA from phage lambda (λ-DNA, Roche) was pre-stained with YOYO-1 (YOYO, Invitrogen) at a ratio of 1 dye molecule per 10 basepairs by mixing at high ionic strength (5× TBE, 445 mM Tris-Borate pH 8.3, 10 mM EDTA, prepared from 10× TBE tablets, Medicago) and incubating at 50°C for 1.5 h to achieve high homogeneity in the staining of the DNA (23). The mixture was subsequently diluted with milliQ water to final concentrations of 0.5× TBE, 1 μM DNA (basepairs) and 0.1 μM YOYO. Pre-stained DNA was then mixed with Cox protein (P2 or WΦ) at the desired molar ratio (DNA:protein 1:1, i.e. equal molar concentrations of DNA basepairs and protein, or 1:0.5, i.e. twice the molar concentration of DNA basepairs compared to protein), incubated at 30°C for 1 h and then kept at room temperature until introduced into the nanofluidic system (1–1.5 h). Both proteins were diluted using the same buffer (20 mM Tris-HCl pH 7.5, 150 mM NaCl, 15% isopropanol and 0.5 mM TCEP) and in samples without protein a corresponding volume of protein buffer was added to ensure as similar buffer conditions as possible in all experiments. The DNA concentration was 0.9 μM (basepairs) in all samples and 3% (v/v) β-mercaptoethanol (Sigma-Aldrich) was added as an oxygen scavenger to suppress oxygen radical induced photodamage of the DNA. For control experiments performed using the P2 genome, P2 phages were prepared as described by Bertani and Bertani (24) and the P2 genome was extracted from the phage particles with phenol, which was later removed by extensive dialysis at 4°C against 10 mM Tris, 1 mM EDTA pH 7.5. Pre-staining of the P2-genome

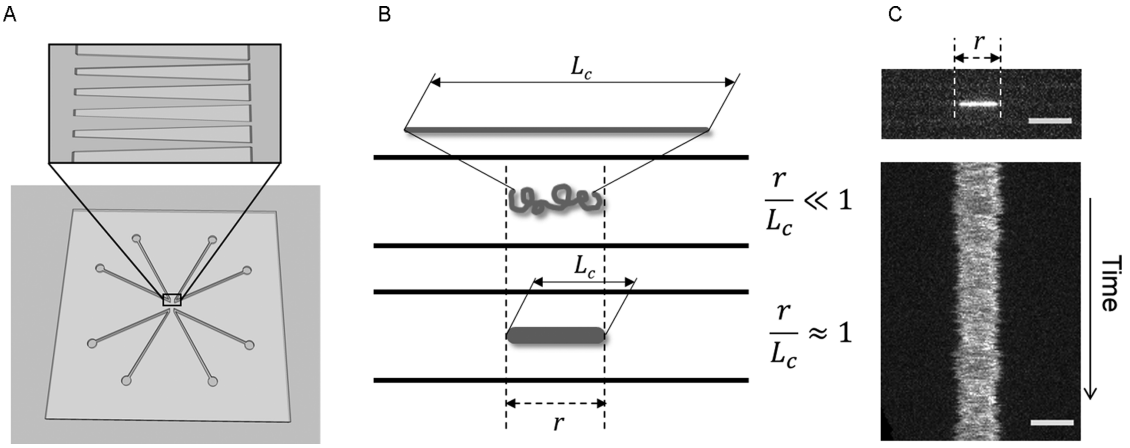

Figure 2. (**A**) Schematic illustration of the nanofluidic chip design, with two separate channel systems on the same chip (bottom). Each channel system comprises pairs of microchannels, spanned by an array of tapered nanochannels, 500 μm long, 140 nm deep and ranging in width from 800 to 100 nm (top). (**B**) A cartoon showing two different polymers confined to a nanochannel. DNA will be only partially stretched out in the nanochannel, with an extension, r, shorter than its contour length, L_c, ($r/L_c << 1$) (top). A stiff polymer confined to a nanochannel will be extended to its full contour length ($r/L_c \approx 1$) (bottom). (**C**) A microscopy image of a single YOYO-stained λ-DNA molecule confined to a 200 × 140 nm^2 nanochannel (top). Stacks of microscopy images can be combined to form a time trace, or kymograph, were each line corresponds to a single frame (bottom). Scale bars in the microscopy images correspond to 5 μm, the cartoons are not drawn to scale.

and sample preparation for nanofluidic experiments was done as described for λ-DNA.

The DNA and DNA–protein complexes were imaged using an epifluorescence microscope (Zeiss AxioObserver.Z1) equipped with a Photometrics Evolve EMCCD camera, a 63× oil immersion TIRF objective (NA = 1.46) and an 1.6× optovar from Zeiss. Using the microscopy imaging software ZEN, 200 subsequent images were recorded with an exposure time of 100 ms and approximately seven images per second.

Data analysis was performed using a custom-written MatLab-based software. The microscopy image stacks were used as input to the software and converted into kymographs (time traces, Figure 2C). From the kymographs extensions and intensities, with standard deviations, were extracted for each molecule (or molecular complex) (25).

AFM

For the AFM studies, we used 1 kbp NoLimits DNA (Fisher Scientific). The AFM images were recorded in air, with a Dimension ICON scanning probe microscope (Bruker) operating in peak force tapping mode. SCANASYST-AIR probes (Bruker) with a spring constant of 0.2 N/m were used. The tapping frequency was 70 kHz and the scanning rate was 0.7 Hz. Samples were prepared by depositing 10 μl of sample solution, either DNA (0.1 μM in basepairs) or DNA (0.1 μM in basepairs) incubated at 30°C for 1 h with P2 Cox at a molar ratio of 1:0.5 (DNA basepairs:protein), on a freshly cleaved mica surface. The sample was left on the mica surface for 5 min, whereafter rinsing was done by gently applying mQ water on the mica surface. Excess mQ was removed with a tissue before drying the surface properly with nitrogen gas.

RESULTS AND DISCUSSION

To investigate how the two Cox homologs from bacteriophages P2 and WΦ affect the physical properties of DNA, we mixed protein and pre-stained DNA at different binding ratios and observed individual complexes at a channel dimension of 200 × 140 nm^2. Since the proteins are not fluorescently labeled we used the fluorescent dye YOYO-1 (YOYO), a well-characterized fluorophore that binds to DNA by bis-intercalating its two aromatic subunits between the DNA-basepairs, to visualize the DNA (23). A prerequisite for studying effects on DNA, caused by interactions with non-labeled proteins, on the single molecule level, is the use of a monodisperse DNA that is well defined in length. Long DNA is preferred, especially when, as in this case, the DNA is strongly compacted and the resulting complexes are small. We therefore used λ-DNA (48 500 basepairs) as model DNA in this study. Control experiments were performed with P2 Cox on the actual phage P2 genome to verify that the results obtained with the model DNA are adequate (Supplementary Figure S1). The observations made with λ-DNA were similar to those made with the phage P2 genome, justifying the use of λ-DNA as a model DNA. Both genomes are compacted to a similar extent, slightly more for the P2 DNA, upon addition of P2 Cox.

Cox compacts DNA and binding is cooperative

The DNA–Cox complexes, as well as naked DNA, confined to nanochannels were imaged by fluorescence microscopy and the extensions (r, see Figure 2B) and emission intensities were extracted from the image stacks (Figure 2C). Figure 3 shows the extension of the DNA–protein complexes at different DNA:protein ratios compared with that of naked DNA. Note that the extension of naked DNA at this confinement and buffer condition is about 4.3 μm, approximately a quarter of its contour length (L_c, see Figure 2B, 16 μm for λ-DNA). The average extension of the DNA de-

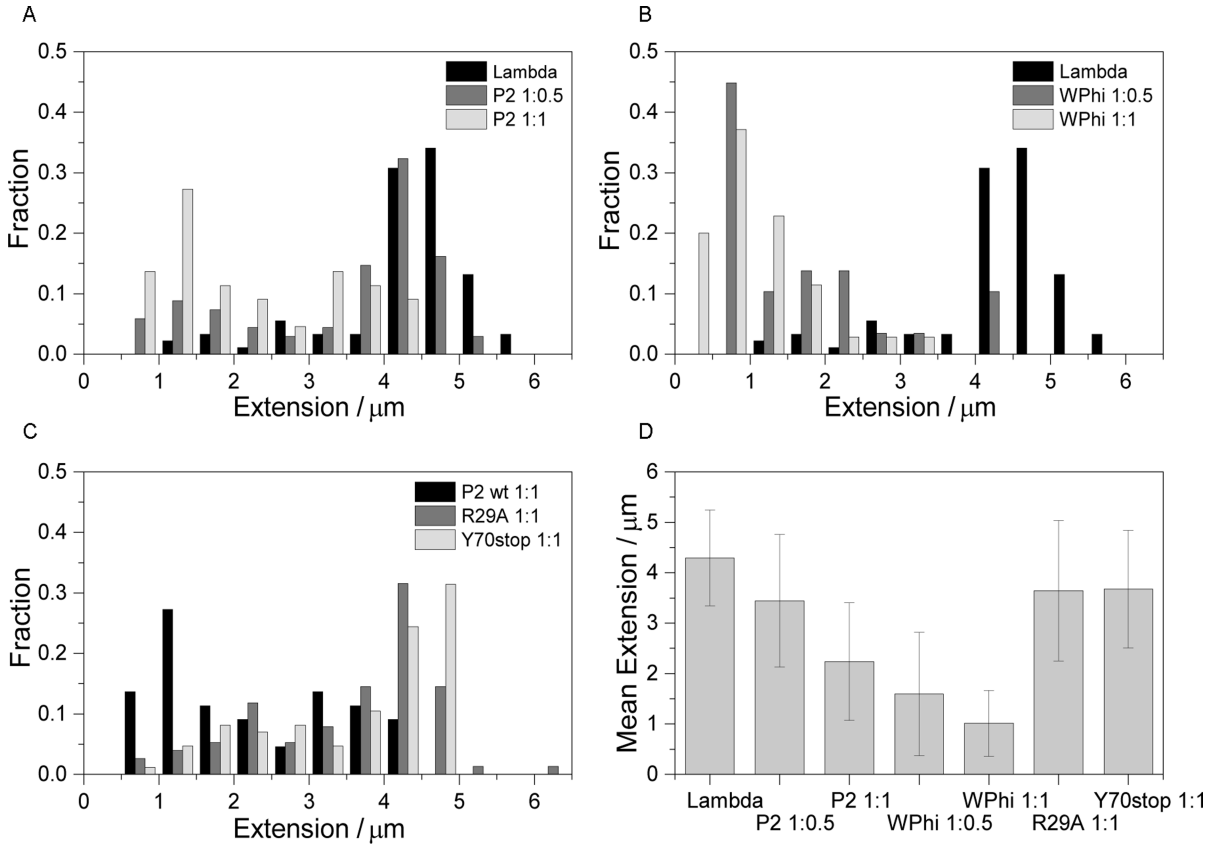

Figure 3. Extension of DNA confined to nanochannels of 200 nm width. (**A**)-(**B**) In absence (black) or presence of Cox from either P2 (A) or WΦ (B) at indicated molar ratios (DNA basepairs:protein). (**C**) In presence of wild-type P2 Cox (black) or any of the mutants R29A or Y70stop. (**D**) Mean values with standard deviations for all combinations of protein and DNA. The number of molecules investigated was $n = 91$ for λ-DNA, $n = 68$ for P2 1:0.5, $n = 44$ for P2 1:1, $n = 29$ for WΦ 1:0.5, $n = 35$ for WΦ 1:1, $n = 77$ for R29A and $n = 86$ for Y70stop.

creases in presence of Cox from both P2 and WΦ, indicating that the protein compacts the DNA. When increasing the protein concentration, the DNA becomes more compacted. Figure 3 also shows that WΦ Cox compacts DNA to a higher extent than P2 Cox does at the same protein concentration. When the protein concentration is increased even further, all complexes are short and hence strongly compacted (Supplementary Figure S2). There is a wider distribution of extensions when the protein is present than for naked DNA, as seen in the histograms in Figures 3A and B and indicated by the larger standard deviations of the mean extension (Figure 3D). This means that while some DNA molecules are fully wrapped around Cox filaments, and therefore compacted to a large extent, others are only sparsely interacting with protein. In turn, this suggests that the binding of Cox to DNA is highly cooperative, which agrees well with previous experiments (7), and with the proposed binding model where multiple Cox monomers form a filament around which DNA can wrap itself (9,10). That the DNA–WΦ Cox complex is more compact than its DNA-P2 Cox counterpart at the same protein concentration can be due to one, or both, of two features of the protein; Either WΦ Cox has a higher affinity to DNA than P2 Cox has, or the WΦ Cox filament is more compact in its structure than the P2 Cox filament.

To understand the compaction process further we in Figures 3C and D include two P2 Cox mutants. In R29A an arginine has been replaced with an alanine, resulting in a decreased affinity for DNA. In Y70stop, the C-terminal tail that is responsible for oligomerization has been deleted (10). Both of these mutants compact DNA to a lesser extent than the wild-type P2 protein (Figures 3C and D). Approximately twice the amount of protein is required to obtain the same degree of compaction for the mutants compared to the wild-type protein.

Visualizing compaction of DNA by P2 Cox using AFM

To confirm the observations made using the nanofluidic channels and fluorescence microscopy, we turned to AFM imaging of DNA. Figure 4 shows AFM images of naked DNA and DNA with P2 Cox bound at a DNA:protein ratio of 1:0.5. The DNA used is 1 kb long (see Materials and Methods for details). We determine the size of this DNA without protein to 0.29 ± 0.04 μm, in agreement with the expected length for 1 kbp B-DNA (26). Cox decreases the contour length of DNA to 0.19 ± 0.05 μm at a DNA:protein ratio of 1:0.5. Thus the compaction is approximately of the same extent as is observed in the nanofluidic experiments.

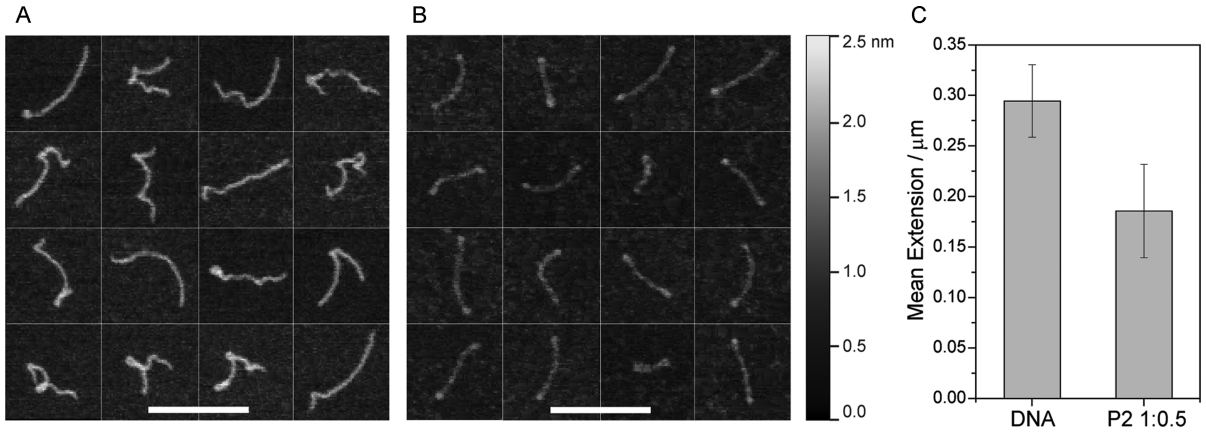

Figure 4. AFM images of DNA (**A**) and of DNA in presence of P2 Cox at a molar ratio of 1:0.5 (DNA basepairs:protein) (**B**), immobilized on mica. The scale bars correspond to 300 nm. (**C**) Average lengths, obtained by tracing the centerline of individual DNA molecules or DNA–protein complexes, for DNA ($n = 32$) and DNA:Cox 1:0.5 ($n = 45$).

Cox-bound DNA exposes its bases to the surrounding solution

That the YOYO dye is bound to the DNA also in presence of the protein is crucial for this study since the protein itself is not labeled. The fact that some dye is still bound at the highest degree of compaction indicates that at least part of the DNA is exposed to the surrounding solution, supporting the hypothesis from our earlier work that the DNA is wrapped on the outside of the protein filament, exposing the DNA basepairs to the solution (10). As described in the Materials and Methods section, the DNA was prestained with YOYO before mixing with protein. Control experiments were performed with the opposite mixing order, verifying the ability of YOYO to bind to Cox-bound DNA (Supplementary Figure S3).

Figure 5 shows the emission intensity for each individual DNA–protein complex as a function of extension. DNA–protein complexes that are significantly compacted have a larger emission intensity per length unit. With preserved dye binding, this is expected for a DNA–protein complex where the DNA is compacted since that yields a complex with more YOYO-stained DNA per pixel, further supporting the hypothesis that Cox compacts DNA. Furthermore, there is a wide distribution of both extensions and emissions for a specific DNA:protein ratio, suggesting that each DNA molecule or DNA-Cox complex is unique. This diversity might be a reflection of the cooperativity in DNA binding by Cox, but can also be due to heterogeneous distribution of YOYO on the DNA (23) and/or that Cox can bind in an unspecific manner, with lower affinity, to the outside of the DNA-protein filament and thus hinder YOYO from binding. There is a clear difference between Cox from the two bacteriophages; YOYO has a higher affinity to the DNA–WΦ Cox complex than the DNA–P2 Cox complex, indicating subtle but significant differences in the binding of DNA to the protein filaments.

Physical properties of DNA–Cox complexes

To investigate the physical properties of the DNA–protein complex further we studied the complexes in nanochannels of varying widths. The use of tapered channels allows us to expose the same individual DNA–protein complex to different degrees of confinement in the same channel. This approach has earlier been shown to be successful for studying DNA itself (22,27) and also for RecA bound to DNA (20). We here measured the extension of DNA-Cox filaments at two channel widths (200 and 600 nm) and calculated the ratio of the extensions at the two confinements. Since we know from above that each individual DNA–protein complex is different, and that the uneven distribution of Cox on the DNA molecules results in data-points in the whole range of extensions in a single sample, we plot the extension ratio versus the extension in the narrow end for each individual complex (Figure 6). Two regions can be identified; at larger extensions, where less protein is bound to the DNA, the extension ratio is constant and very similar to that of DNA alone. At smaller extensions, thus higher degree of compaction and more protein associated to each DNA molecule, the ratio decreases significantly with decreasing extension suggesting that the DNA–protein complex becomes stiffer. A constant extension ratio, as in the region at larger extensions, indicates that the physical properties of the complex are mainly governed by the flexible naked DNA. When the protein filaments get longer, and more of the DNA molecule is protein-bound, the physical properties of the DNA–Cox complex are rather governed by the significantly stiffer Cox filament. It is however difficult to say anything about how stiff the filament is since there likely is additional protein binding on the outside of the DNA-Cox filament. Interestingly, the shape of the curve is very similar for the two Cox homologs. This suggests that the DNA binding mode of the two Cox proteins is similar and that the observed differences between the two proteins discussed above are rather based on a higher affinity to DNA for WΦ Cox than significantly different modes of binding.

For a DNA molecule completely wrapped around a Cox filament we expect a contour length that is approximately seven times shorter than for naked DNA, based on our previous P2 Cox model (10). Naked λ-DNA has a contour length of 16 μm and a fully covered λ-DNA-Cox filament should then be ∼2.3 μm long. The most compact DNA–Cox complexes we observe, at high protein coverage, are as

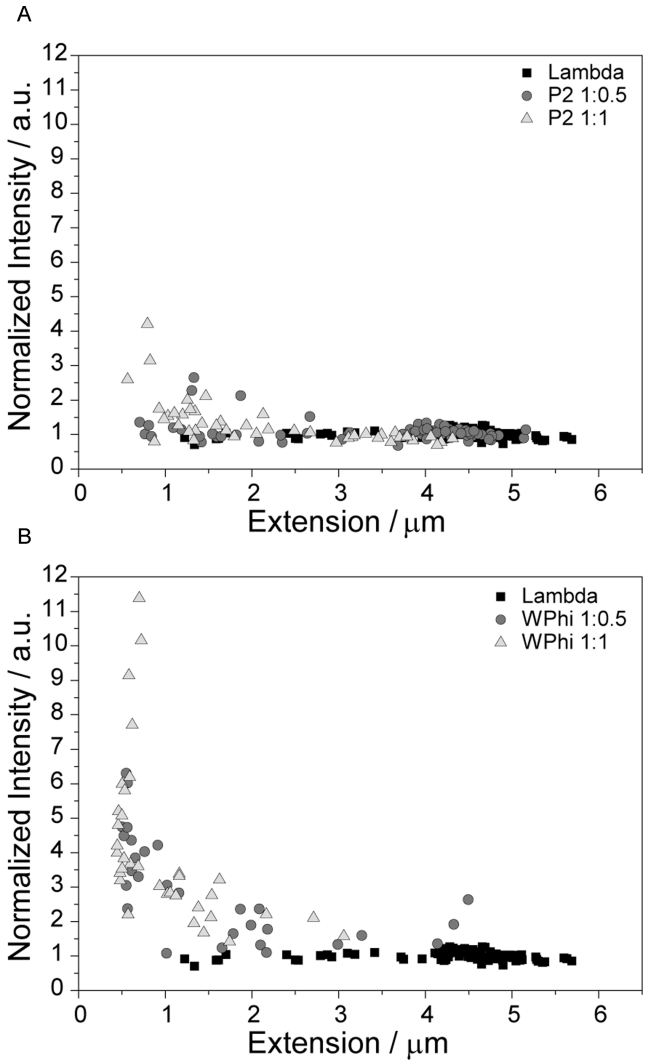

Figure 5. Normalized emission intensity from individual YOYO-stained DNA molecules, in absence (black) or presence of Cox from either P2 (**A**) or WΦ (**B**) in samples mixed at two different binding ratios (DNA basepairs:protein, as indicated). Each data point represents an individual DNA molecule or DNA–protein complex, the average emission intensity for DNA without protein is set to 1 and the rest of the data are normalized relative to that. The molecules were confined at 200 nm channel width.

short as around 0.5 μm in extension (Figure 3) with an extension ratio close to one (Figure 6), indicating that they are stretched to nearly their full contour length. That the complexes are this small suggests that they are 'oversaturated' with protein, most likely protein bound in a second, non-specific, external binding mode. It is reasonable to assume that *in vivo*, the Cox concentration does not reach such high levels or that there is another process regulating the amount of Cox bound. Since Cox is vitally important for both repression and excision activity, it is likely that the organism has a strict regulation on the expression levels of Cox. The exact mechanism for this is however not yet known.

The group of Johan van der Maarel has used nanochannels to study several proteins that compact DNA, such as H-NS and Hfq (17,18). For these proteins they observe a step-like transition from an extended DNA–protein complex to a compact complex with increasing protein concentration, whereas we here see a gradual decrease in extension with increasing Cox concentration. We believe that this discrepancy is related to the fact that H-NS and Hfq bind to DNA stochastically as monomers whereas Cox forms a filament that wraps the DNA and thus has a completely different binding mode.

Local distribution of Cox along the DNA

The fact that we stretch out the DNA–protein complexes in the channels makes it possible to investigate variations in the emission signal along the DNA, similar to what we do in optical DNA mapping (28), and potentially relate that to the distribution of protein along the DNA. Figure 7A shows several kymographs of P2 Cox bound to DNA at molar ratio of 1:0.5. There is a large variation in the appearance of the kymographs of the DNA–protein complexes but from a qualitative assessment (by eye) we estimate that approximately half of the kymographs we have recorded has a significantly higher emission intensity in some region of the extension. This is not observed for DNA without protein added, but the high-intensity regions are common also for complexes formed with WΦ Cox (not shown). Furthermore, a vast majority of these regions are at one of the ends of the DNA molecule. This agrees with AFM experiments (Figure 7B) where we commonly see that the DNA–protein complex is higher in at least one of the ends. We speculate that these are regions where the DNA is wrapped around Cox filaments. To test this hypothesis, we turn to the two mutant proteins. The R29A mutant should form filaments in the same way as the wild-type protein but bind DNA with a lower affinity, while Y70stop cannot form filaments. Interestingly, we see very few DNA–protein complexes with high intensity regions for the Y70stop mutant, in agreement with its lack of capability to form filaments. For R29A on the other hand we observe at least as much high intensity regions as for the wild-type protein. Y70stop still compacts the DNA to some extent (Figure 3D), suggesting that the Cox protein can also compact DNA in its monomeric form. The data collected for the three versions of the protein thus allows us to discriminate between compaction that is due to wrapping of the DNA around a Cox filament and compaction that is due to monomeric protein binding. We are also able to conclude that the filaments preferably bind to the end of the DNA. It is worth pointing out that in the P2 and WΦ phage genomes there are specific binding sites, with a defined sequence, that direct the Cox proteins to where binding should be initiated and also in which direction the DNA–protein complex is formed (2).

CONCLUSION

To conclude, we have here demonstrated, using nanofluidic channels and AFM, that both P2 Cox and WΦ Cox compact DNA upon binding, corroborating our previous DNA-P2 Cox binding model. Furthermore, we have shown that the DNA binding is highly cooperative, in line with the model of DNA wrapped around a filament of protein oligomers. The two DNA–Cox complexes display similar physical properties, which at low protein concentrations are

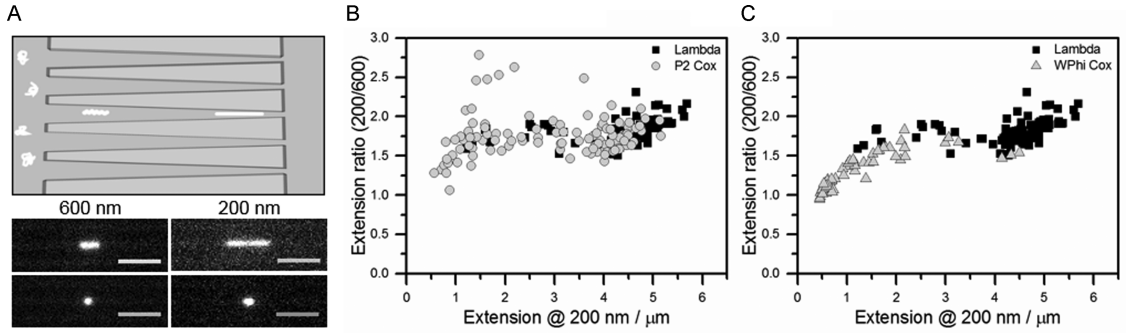

Figure 6. (**A**) A schematic outline of the nanofunnels used in this study, illustrating DNA molecules in a coiled conformation in a microchannel and successively stretched out when brought into a nanofunnel (top). Below are microscopy images of two single YOYO-stained DNA molecules in presence of P2 Cox, mixed at a molar ratio of 1:1 (DNA basepairs:protein), confined to a nanofunnel and positioned at a width of 600 nm (left) and 200 nm (right), respectively. The molecule imaged in the lower panel has more protein bound, compared to the molecule in the upper panel, and is thus more compacted and more stiff. Scale bars in the microscopy images correspond to 5 μm, the cartoon is not drawn to scale. (**B**) and (**C**) The ratio between the extension of individual DNA molecules, in absence (black) or presence of Cox from either P2 (B) or WΦ (C), at a width of 200 and 600 nm in a 140 nm deep nanofunnel.

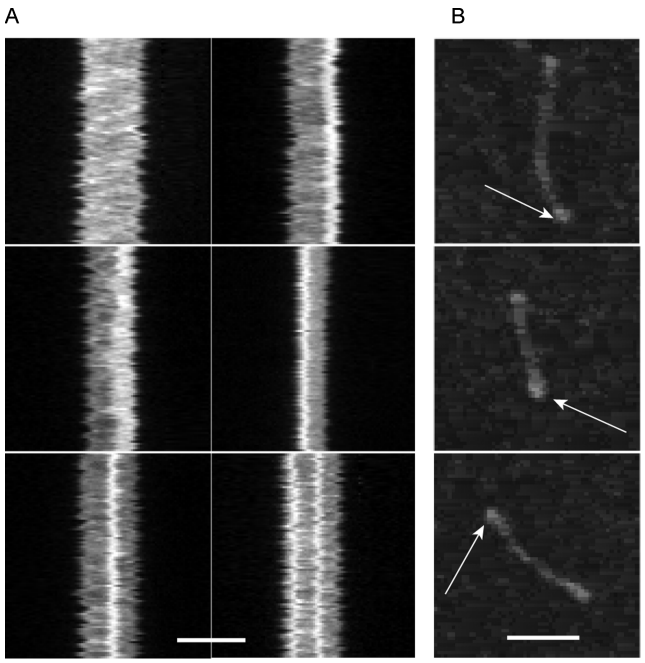

Figure 7. Examples of typical kymographs (**A**) and AFM images (**B**) for DNA–protein complexes with P2 Cox at a molar ratio of 1:0.5 (DNA basepairs:protein). The scale bar corresponds to 5 μm in (A) and 200 nm in (B). The arrows in (B) point out regions where the complex displays a larger height, believed to be parts of the DNA compacted by Cox.

unaffected when comparing with naked DNA, but at increasing protein coverage become more governed by the stiffer protein filament. We suggest that subtle differences detected between P2 and WΦ Cox are due to a difference in binding affinity to DNA for the two proteins rather than a difference in binding mode. Using P2 Cox mutants with known effects on DNA binding we are also able to directly visualize the DNA wound up around protein filaments and distinguish between compaction due to filament formation and compaction by monomeric Cox. This work highlights the possibilities of using stretching of single DNA molecules in nanofluidic channels to confirm structural predictions from X-ray crystallography. Nanofluidic channels allow high throughput and the heterogeneous binding of Cox to DNA makes it possible to study many DNA:protein ratios in the same sample.

SUPPLEMENTARY DATA

Supplementary Data are available at NAR Online.

ACKNOWLEDGEMENTS

The group of Assoc. Prof. Tobias Ambjörnsson at Lund University is acknowledged for developing the data analysis software. Erik Werner is acknowledged for fruitful discussions. Karin Skaar is acknowledged for technical assistance.

FUNDING

Swedish Research Council [project 2011–4324 to F.W., projects 2010–5200, 2014–5667 to P.S.]; Chalmers Area of Advance in Nanoscience and Nanotechnology [to F.W.]; Wenner-Gren Foundation [to P.S.]; Carl Tryggers Foundation [to P.S.]; EMBO Long Term Fellowship; Marie Curie Actions EMBOCOFUND2010 [GA-2010- 267146 to R. B]. Funding for open access charge: Swedish Research Council.
Conflict of interest statement. None declared.

REFERENCES

1. Bertani,G. and Six,E.W. (1988) In: Calender,R (ed). *The P2-like phages and their parasite, P4*. Plenum Publishing Corp, NY.
2. Nilsson,A.S. and Haggård-Ljungquist,E. (2006) The P2-like bacteriophages. In: Calender,R (ed). *The Bacteriophages*. Oxford University Press, NY.
3. Massad,T., Skaar,K., Nilsson,H., Damberg,P., Henriksson-Peltola,P., Haggard-Ljungquist,E., Hogbom,M. and Stenmark,P. (2010) Crystal structure of the P2 C-repressor: a binder of non-palindromic direct DNA repeats. *Nucleic Acids Res.*, **38**, 7778–7790.
4. Yu,A. and Haggård-Ljungquist,E. (1993) The Cox protein is a modulator of directionality in bacteriophage P2 site-specific recombination. *J. Bacteriol.*, **175**, 7848–7855.
5. Saha,S., Haggård-Ljungquist,E. and Nordström,K. (1987) The cox protein of bacteriophage P2 inhibits the formation of the repressor protein and autoregulates the early operon. *EMBO J.*, **6**, 3191.

6. Saha,S., Haggård-Ljungquist,E. and Nordström,K. (1989) Activation of prophage P4 by the P2 Cox protein and the sites of action of the Cox protein on the two phage genomes. *Proc. Natl. Acad. Sci. U.S.A.*, **86**, 3973–3977.
7. Ahlgren-Berg,A., Cardoso-Palacios,C., Eriksson,J.M., Mandali,S., Sehlén,W., Sylwan,L. and Haggård-Ljungquist,E. (2009) A comparative analysis of the bifunctional Cox proteins of two heteroimmune P2-like phages with different host integration sites. *Virology*, **385**, 303–312.
8. Liu,T. and Haggård-Ljungquist,E. (1999) The transcriptional switch of bacteriophage WΦ, a P2-related but heteroimmune coliphage. *J. Virol.*, **73**, 9816–9826.
9. Eriksson,J.M. and Haggård-Ljungquist,E. (2000) The multifunctional bacteriophage P2 cox protein requires oligomerization for biological activity. *J. Bacteriol.*, **182**, 6714–6723.
10. Berntsson,R.P.A., Odegrip,R., Sehlen,W., Skaar,K., Svensson,L.M., Massad,T., Hogbom,M., Haggard-Ljungquist,E. and Stenmark,P. (2014) Structural insight into DNA binding and oligomerization of the multifunctional Cox protein of bacteriophage P2. *Nucleic Acids Res.*, **42**, 2725–2735.
11. Levy,S.L. and Craighead,H.G. (2010) DNA manipulation, sorting, and mapping in nanofluidic systems. *Chem. Soc. Rev.*, **39**, 1133–1152.
12. Persson,F. and Tegenfeldt,J.O. (2010) DNA in nanochannels—directly visualizing genomic information. *Chem. Soc. Rev.*, **39**, 985.
13. Reisner,W., Pedersen,J.N. and Austin,R.H. (2012) DNA confinement in nanochannels: physics and biological applications. *Rep. Prog. Phys.*, **75**, 106601.
14. Nyberg,L.K., Persson,F., Berg,J., Bergström,J., Fransson,E., Olsson,L., Persson,M., Stålnacke,A., Wigenius,J., Tegenfeldt,J.O. *et al.* (2012) A single-step competitive binding assay for mapping of single DNA molecules. *Biochem. Biophys. Res. Commun.*, **417**, 404–408.
15. Lam,E.T., Hastie,A., Lin,C., Ehrlich,D., Das,S.K., Austin,M.D., Deshpande,P., Cao,H., Nagarajan,N., Xiao,M. *et al.* (2012) Genome mapping on nanochannel arrays for structural variation analysis and sequence assembly. *Nat. Biotechnol.*, **30**, 771–776.
16. Persson,F., Fritzsche,J., Mir,K.U., Modesti,M., Westerlund,F. and Tegenfeldt,J.O. (2012) Lipid-based passivation in nanofluidics. *Nano Lett.*, **12**, 2260–2265.
17. Zhang,C., Guttula,D., Liu,F., Malar,P.P., Ng,S.Y., Dai,L., Doyle,P.S., van Kan,J.A. and van der Maarel,J.R.C. (2013) Effect of H-NS on the elongation and compaction of single DNA molecules in a nanospace. *Soft Matter*, **9**, 9593–9601.
18. Jiang,K., Zhang,C., Guttula,D., Liu,F., Van Kan,J.A., Lavelle,C., Kubiak,K., Malabirade,A., Lapp,A., Arluison,V. *et al.* (2015) Effects of Hfq on the conformation and compaction of DNA. *Nucleic Acids Res.*, **43**, 4332–4341.
19. Streng,D.E., Lim,S.F., Pan,J., Karpusenka,A. and Riehn,R. (2009) Stretching chromatin through confinement. *Lab on a Chip*, **9**, 2772.
20. Frykholm,K., Alizadehheidari,M., Fritzsche,J., Wigenius,J., Modesti,M., Persson,F. and Westerlund,F. (2014) Probing Physical Properties of a DNA–protein complex Using Nanofluidic Channels. *Small*, **10**, 884–887.
21. Studier,F.W. and Moffatt,B.A. (1986) Use of bacteriophage T7 RNA polymerase to direct selective high-level expression of cloned genes. *J. Mol. Biol.*, **189**, 113–130.
22. Persson,F., Utko,P., Reisner,W., Larsen,N.B. and Kristensen,A. (2009) Confinement spectroscopy: probing single dna molecules with tapered nanochannels. *Nano Lett.*, **9**, 1382–1385.
23. Nyberg,L., Persson,F., Åkerman,B. and Westerlund,F. (2013) Heterogeneous staining: a tool for studies of how fluorescent dyes affect the physical properties of DNA. *Nucleic Acids Res.*, **41**, e184–e184.
24. Bertani,L.E. and Bertani,G. (1970) Preparation and characterization of temperate, non-inducible bacteriophage P2 (host: *Escherichia coli*). *J. Gen. Virol.*, **6**, 201–212.
25. Frykholm,K., Nyberg,L.K., Lagerstedt,E., Noble,C., Fritzsche,J., Karami,N., Ambjörnsson,T., Sandegren,L. and Westerlund,F. (2015) Fast size-determination of intact bacterial plasmids using nanofluidic channels. *Lab on a Chip*, **15**, 2739–2743.
26. Wing,R., Drew,H., Takano,T., Broka,C., Tanaka,S., Itakura,K. and Dickerson,R.E. (1980) Crystal-structure analysis of a complete turn of b-Dna. *Nature*, **287**, 755–758.
27. Westerlund,F., Persson,F., Kristensen,A. and Tegenfeldt,J.O. (2010) Fluorescence enhancement of single DNA molecules confined in Si/SiO2 nanochannels. *Lab on a Chip*, **10**, 2049–2051.
28. Nilsson,A.N., Emilsson,G., Nyberg,L.K., Noble,C., Stadler,L.S., Fritzsche,J., Moore,E.R.B., Tegenfeldt,J.O., Ambjornsson,T. and Westerlund,F. (2014) Competitive binding-based optical DNA mapping for fast identification of bacteria - multi-ligand transfer matrix theory and experimental applications on Escherichia coli. *Nucleic Acids Res.*, **42**, e118.